A Fully Distributed Dual Consensus ADMM Based on Partition for DC-OPF with Carbon Emission Trading

Linfeng Yang, Jiangyao Luo, Yan Xu, *Member*, *IEEE*, Zhenrong Zhang, Zhaoyang Dong, *Fellow*, *IEEE*

***Abstract*—This paper presents a novel fully distributed alternating direction method of multipliers (ADMM) approach for solving the direct current optimal power flow with carbon emission trading (DC-OPF-CET) problem. Different from the other ADMM-based distributed approaches which disclosing boundary buses and branches information among adjacent subsystems, our proposed method adopts a new strategy by using ADMM to solve the dual of DC-OPF-CET, making it only needs disclosing boundary branches information among adjacent subsystems. We improve convergence speed of our method further by reducing the coupling constraints and employing an improved update step of multiplier. The proposed method was tested on cases ranging from 6 to 600 buses. The simulation results show that our proposed distributed method can solve the DC-OPF-CET efficiently and its convergence speed can be improved by reducing coupling constraints and employing new update strategy for multiplier.**

***Index Terms*—ADMM, dual, partition, distributed DC-OPF, carbon emission trading.**

NOMENCLATURE

Operator:

$[\cdot]^-$	$\min(0,\cdot)$
$[\cdot]^+$	$\max(0,\cdot)$
$\lvert\cdot\rvert$	Number of elements in "·", if "·" is a set.

Indices:

i	Index for unit/bus.
t	Index for time period.

Constants:

S^{B}	Set of buses, $\lvert S^{\mathrm{B}}\rvert = N$ and $S^{\mathrm{B}} = \{1, \dots, N\}$.
S^{G}	Set of buses with units. $\lvert S^{\mathrm{G}}\rvert = G$ and $S^{\mathrm{G}} \subseteq S^{\mathrm{B}}$.
S^{TP}	Set of time periods, and $\lvert S^{\mathrm{TP}}\rvert = T$.
S^{L}	Set of lines, and $\lvert S^{\mathrm{L}}\rvert = L$.
S^{ref}	Set of reference bus.
$\alpha_i, \beta_i, \gamma_i$	Coefficients of the quadratic production cost function of unit i.
a_i, b_i, c_i	Coefficients of the quadratic emission function of unit i.
π_{b}, π_{s}	Price of emission allowances bought or sold on the market.
$F_{ij}^{\max}$	Maximum power flow limit on line ij.
X_{ij}	Reactance of line ij.
$\underline{P}_i^{\mathrm{G}}$	Minimum power output of unit i.
$\bar{P}_i^{\mathrm{G}}$	Maximum power output of unit i.
$P_{i,t}^{\mathrm{D}}$	System load demand on bus i in time period t.
$P_i^{\mathrm{G,up}}$	Ramp up limit of unit i.
$P_i^{\mathrm{G,down}}$	Ramp down limit of unit i.
$\boldsymbol{e}$	Vector with all components one.
$\boldsymbol{0}$	Matrix with all components zero.
$\boldsymbol{B}$	Network admittance matrix ($\Re^{N\times N}$).
B_{ij}	Element of $\boldsymbol{B}$ in the i^{th} row and j^{th} col.
E_0	The total emission allowance of CO_2.
$\Delta E_{\mathrm{b}}^{\max}$	The maximum emission allowances which can be bought on the market.
$\Delta E_{\mathrm{s}}^{\max}$	The maximum emission allowances which can be sold on the market.
μ	Coefficients of the update step for multiplier.

Variables:

$P_{i,t}^{\mathrm{G}}$	Power output of unit on bus i in time period t.
$\theta_{i,t}$	Phase angle on bus i in time period t.
ΔE_{b}, ΔE_{s}	Amount of emission allowances bought and sold on the market.

I. INTRODUCTION

Optimal power flow (OPF) is one of the fundamental problems in the power systems and it aims to minimize the generation cost subject to some constraints, e.g. bus voltage limits, unit constraints and bus power limits, etc. The idea of using a unified model to consider the aforementioned concerns was introduced by Carpentier in 1962 [1]. Under some assumptions such as small voltage phase angles, alternating current optimal power flow (AC-OPF) is approximately to direct current optimal power flow (DC-OPF) for obtaining the optimal dispatch solution of the entire power system.

A vast amount of approach has been done on OPF solution methods in conventional centralized power system with one control entity [2]-[4]. For the centralized OPF, all data have to be transferred to and processed in the central controller. In actually, distribution region in a power network may belong to different owners, they might refuse to share some data because of security concerns. The distributed OPF exactly guarantee the privacy of information since adjacent subsystems exchange only a limited amount of information relating to boundary branches or boundary buses, which is in fact one of the targets of distributed OPF [5]. Thus, individual subsystems do not need to disclose their confidential information/parameters to other subsystems [7]. The distributed approach is often computationally more expensive than the centralized approach but en-

This work was supported by the Natural Science Foundation of China (51767003, 11771383, 61661004), the Guangxi Key Laboratory of Power System Optimization and Energy Technology Foundation (15-A-01-11).

L.F. Yang, the corresponding author, is with the School of Computer Electronics and Information, Guangxi University, Nanning 530004, China, and also with the Guangxi Key Laboratory of Power System Optimization and Energy Technology, Guangxi University. (e-mail: ylf@gxu.edu.cn).

J.Y. Luo is with the School of Computer Electronics and Information, Guangxi University, Nanning 530004, China.

Y. Xu is with School of Electrical and Electronic Engineering, Nanyang Technological University, Singapore 639798 (e-mail: yan.xu@sydney.edu.au).

Z.R. Zhang, the joint corresponding author, is with the Guangxi Key Laboratory of Multimedia Communications and Network Technology, Nanning 530004, China. (e-mail: zzr76@gxu.edu.cn)

Z.Y. Dong is with the School of Electrical Engineering and Tele-communications, The University of NSW, Sydney, NSW 2052, Australia. (e-mail: zydong@ieee.org).

able the independent operation of each interconnected subsystem while the global optimum is also achieved. In addition, some distributed OPFs can be solved asynchronously via individual local controllers [8].

Over the past few years, a vast amount of research has been explored in distributed methods of OPF [5]-[27]. These methods can be broadly classified into the following categories [6]: analytical target cascading (ATC) [9], [10], auxiliary problem principle (APP) [11], [12], optimality condition decomposition (OCD) [13]-[15], consensus+innovations (C+I) [16], [17], methods based on alternating direction method of multipliers (ADMM) [5], [7], [18]-[24], and some other methods which do not fall into any of the aforementioned categories [25], [26].

The ADMM is well suited to distributed convex optimization, and in particular to large-scale problems [28]. The method was developed in the 1970s, with roots in the 1950s [29]. It can be viewed as an attempt to blend the benefits of dual decomposition and augmented Lagrangian methods for constrained optimization. And it is interesting to note that with no tuning, ADMM can be competitive with the best known methods for some problems. In [18], paper introduced the general form of ADMM, and extends the 2-block ADMM to *N*-block ADMM. Moreover, paper focus on two distributed parallel ADMM-based optimization algorithms: Consensus ADMM and Proximal Jacobian ADMM. The numerical results of Consensus ADMM and Proximal Jacobian ADMM in DC-OPF shows ADMM are suitable to be implemented as distributed parallel algorithms for power networks. A fully distributed consensus-based ADMM without the central controller is proposed in [7] for DC-OPF. This method employs a new communication strategy, which are coordinated via global consensus variables, i.e., phase angels on boundary buses of adjacent subsystem. In [19], a distributed OPF is proposed based on ADMM combined with sequential convex approximations. The centralized OPF is decomposed into subproblems corresponding to each bus, where solutions of the subproblems are coordinated with a light communication protocol among the buses. An ADMM-based algorithm has been applied to the OPF in [20]. In this approach, the power grid is first split into a bipartite graph consisting of devices, nets, and terminals connecting the former two entities. Estimated values for power injections and voltage angles for devices and nodes at a particular iteration, called messages, are then exchanged between neighboring nodes and devices. References [5] and [21] present decentralized OPF algorithms using ADMM, where subproblems directly communicate with each other with no need of a central coordinator.

In general, dividing the whole OPF problem to be region-based or component-based subsystems is a common scheme for ADMM-based distributed methods. At each iteration, each subproblem (i.e., the corresponding decomposed augmented function for each subsystem) is only minimized with respect to a subset of primal variables over which it is decomposed. However, besides the information (such as admittances of buses and branches, etc.) belonging to its own subsystem, this subproblem always need some information of its adjacent subsystems. And we regard this additional information as "public information". For all we know, the existing ADMM-based OPF methods, even most other distributed methods, need taking boundary buses and branches information between all adjacent subsystems as public information.

Different from other popular ADMM-based methods, our proposed approach can reduce the amount of public information by employing ADMM to solve the dual problem. In addition, operating at absolute minimum cost is no longer the only condition for electric power generation due to the pressing public demand for cleaner air [30]. So we introduce carbon emission trading (CET) which facilitates the reduction in greenhouse gas emission while optimizing the daily operation cost of electric power systems.

The major contributions that differentiate our method from other existing methods are the following.

1) Our proposed algorithm only needs disclosing *public boundary branches* information among adjacent subsystems while most other ADMM-based methods need disclosing *private boundary buses* information among adjacent subsystems on the basis of our algorithm. Simply, the volume of public information of our proposed algorithm is much smaller.

2) In our method, the number of elements in consensus variable is only determined by the number of coupling constraints in DC-OPF with CET (DC-OPF-CET) problem. We improved the convergence speed of the proposed method by identifying the uncoupled buses and reducing the number of coupling constraints.

3) We employed a new update strategy for multiplier given in [31] to reduce the number of iterations of our method further.

4) By setting the partition set, theoretically, our method can divide DC-OPF-CET arbitrarily to be multiple subsystems, even to be a series of single buses. And all information in the right hand side (RHS) of constraints can be arranged arbitrarily to any subsystems and be kept secret from the other subsystems.

The organization of this paper is arranged as follows. Section II presents the mathematical formulation of DC-OPF-CET. The proposed fully distributed DC-OPF-CET approach and several discussions about reducing coupling constraints, public information, and improved update strategy for multiplier are given in Section III. Numerical case studies are presented in Section IV. Finally, a summary are provided in Section V.

II. Mathematical Formulation of DC-OPF-CET

A. Objective Function

The objective of operational planning for DC-OPF-CET is to minimize the total operation cost F_{TC},

$$F_{\mathrm{TC}} = F_{\mathrm{TH}} + F_{\mathrm{CET}}$$

where F_{TH} is the fuel cost of thermal units and F_{CET} is the carbon emissions trading cost.

1) Fuel cost of thermal units (F_{TH})

The fuel cost of thermal units has the form

$$F_{\mathrm{TH}} = \sum_{i\in S^{\mathrm{G}}} \sum_{t\in S^{\mathrm{TP}}} f_i(P_{i,t}^{\mathrm{G}}) \tag{1}$$

where the production cost for unit i can be represented as a quadratic function $f_i(\cdot)$, which is

$$f_i(P_{i,t}^{\mathrm{G}}) = \alpha_i + \beta_i P_{i,t}^{\mathrm{G}} + \gamma_i \left(P_{i,t}^{\mathrm{G}}\right)^2 \tag{2}$$

2) Cost of CET (F_{CET})

CET system is a cap-and-trade market mechanism that has been introduced in European Union in order to facilitate emissions management. In this scheme, usually, a certain amount of allowances, also can be called quota, is given in advance. And this quota can use to cover emissions produced during energy generation [32]. Under CET, emission quota has the property of the goods and power producer has an opportunity to buy and sell emission quotas on the market [33], [34]. In this paper, we assume that the emission quota for DC-OPF-CET is E_0, the actual total emission may be greater or lower than the cap, because of the quota trades. And cost caused in this trading is

$$F_{\mathrm{CET}} = \pi_{\mathrm{b}}\Delta E_{\mathrm{b}} - \pi_{\mathrm{s}}\Delta E_{\mathrm{s}}. \tag{3}$$

B. Constraints

$$P_{i,t}^{\mathrm{G}} - P_{i,t}^{\mathrm{D}} = \sum_{j\in S_{\mathrm{B}}} B_{ij}\theta_{j,t}, \forall t \in S^{\mathrm{TP}}, \forall i \in S^{\mathrm{B}} \tag{4}$$

$$\left|\frac{\theta_{i,t}-\theta_{j,t}}{x_{ij}}\right| \le F_{ij}^{\max}, \forall t \in S^{\mathrm{TP}}, \forall i,j \in S^{\mathrm{B}}, \forall ij \in S^{\mathrm{L}} \tag{5}$$

$$\theta_{i,t} = 0, \forall i \in S^{\mathrm{ref}}, \forall t \in S^{\mathrm{TP}} \tag{6}$$

$$P_{i,t}^{\mathrm{G}} = 0, \forall i \in S^{\mathrm{B}} - S^{\mathrm{G}}, \forall t \in S^{\mathrm{TP}} \tag{7}$$

$$\underline{P_i^{\mathrm{G}}} \le P_{i,t}^{\mathrm{G}} \le \bar{P}_i^{\mathrm{G}}, \forall i \in S^{\mathrm{G}}, \forall t \in S^{\mathrm{TP}} \tag{8}$$

$$P_{i,t}^{\mathrm{G}} - P_{i,t-1}^{\mathrm{G}} \le P_i^{\mathrm{G,up}}, \forall i \in S^{\mathrm{G}}, \forall t \in S^{\mathrm{TP}} \tag{9}$$

$$P_{i,t-1}^{\mathrm{G}} - P_{i,t}^{\mathrm{G}} \le P_i^{\mathrm{G,down}}, \forall i \in S^{\mathrm{G}}, \forall t \in S^{\mathrm{TP}} \tag{10}$$

$$\sum_{i\in S^{\mathrm{G}}}\sum_{t\in S^{\mathrm{TP}}} E_i(P_{i,t}^{\mathrm{G}}) \le E_0 + \Delta E_{\mathrm{b}} - \Delta E_{\mathrm{s}}, \tag{11}$$

$$0 \le \Delta E_{\mathrm{b}} \le \Delta E_{\mathrm{b}}^{\max}, \tag{12}$$

$$0 \le \Delta E_{\mathrm{s}} \le \Delta E_{\mathrm{s}}^{\max}, \tag{13}$$

where $E_i\left(P_{i,t}^{\mathrm{G}}\right) = a_i + b_i P_{i,t}^{\mathrm{G}} + c_i\left(P_{i,t}^{\mathrm{G}}\right)^2$ is emission function. (4) represents the nodal power balance restriction via the direct current (DC) power flow calculation. (5) and (8) are capacity limits of transmission lines and generators. (6) defines the reference bus. (7) represents the buses without generators. (9) -(10) enforce ramp up/down limits of individual generators. (11) restricts the total emission, (12) and (13) give the maximum emission allowances can be bought or sold on the market.

III. Dual Consensus ADMM Based on Partition

A. Description of the Model for our method

For the sake of convenience, throughout the paper, the following notations are used for the DC-OPF-CET problem. $\boldsymbol{P}_i^{\mathrm{G}} = \left[P_{i,1}^{\mathrm{G}}; P_{i,2}^{\mathrm{G}}; \dots; P_{i,T}^{\mathrm{G}}\right]$, $\boldsymbol{P}_i^{\mathrm{D}} = \left[P_{i,1}^{\mathrm{D}}; P_{i,2}^{\mathrm{D}}; \dots; P_{i,T}^{\mathrm{D}}\right]$, $\boldsymbol{P}^{\mathrm{D}} = [\boldsymbol{P}_1^{\mathrm{D}}; \boldsymbol{P}_2^{\mathrm{D}}; \dots; \boldsymbol{P}_N^{\mathrm{D}}]$, $\boldsymbol{\theta}_i = \left[\theta_{i,1}; \theta_{i,2}; \dots; \theta_{i,T}\right]$.

Then the constraints (4) and (5) can be reformulated as

$$\boldsymbol{P}_i^{\mathrm{G}} - \boldsymbol{P}_i^{\mathrm{D}} = \sum_{j\in S^{\mathrm{B}}} B_{ij}\boldsymbol{\theta}_j, \forall i \in S^{\mathrm{B}}, \tag{14}$$

$$-F_{ij}^{\max}\boldsymbol{e} \le \frac{\boldsymbol{\theta}_i - \boldsymbol{\theta}_j}{x_{ij}} \le F_{ij}^{\max}\boldsymbol{e}, \forall ij \in S^{\mathrm{L}},\ i,j \in S^{\mathrm{B}}. \tag{15}$$

Let $x_i = [\boldsymbol{P}_i^{\mathrm{G}}; \boldsymbol{\theta}_i]$, $b_{\mathrm{PF}} = \boldsymbol{P}^{\mathrm{D}}$, $\tilde{A}_i = [\boldsymbol{0}, -B_{1i}\boldsymbol{I}; \cdots; \boldsymbol{I}, -B_{ii}\boldsymbol{I}; \cdots; \boldsymbol{0}, -B_{Ni}\boldsymbol{I}]$, then (14) can be reformulated as $\sum_{i\in S^{\mathrm{B}}} \tilde{A}_i x_i = b_{\mathrm{PF}}$. Similarly, (15) can be reformulated as $\sum_{i\in S^{\mathrm{B}}} \widetilde{M}_i x_i \le b_{\mathrm{BR}}$, where $\widetilde{M}_i$ is coefficient matrix for x_i, b_{BR} is constant vector.

In addition, it can be seen that the constraints (6)-(10) can be fully decoupled according to each unit. Then, for $i \in S^{\mathrm{B}}$, we define $\chi_i = \{x_i | (6) - (10)\}$. For $i \in S^{\mathrm{G}}$, let $g_i(x_i) = \sum_{t\in S^{\mathrm{T}}} f_i\left(P_{i,t}^{\mathrm{G}}\right)$, $\tilde{h}_i(x_i) = \sum_{t\in S^{\mathrm{T}}} E_i\left(P_{i,t}^{\mathrm{G}}\right)$. For $i \in S^{\mathrm{B}} - S^{\mathrm{G}}$, let $g_i(x_i) = \tilde{h}_i(x_i) = 0$. Then the DC-OPF-CET model can be reformulated as

$$\min \sum_{i\in S^{\mathrm{B}}} g_i(x_i) + \pi_{\mathrm{b}}\Delta E_{\mathrm{b}} - \pi_{\mathrm{s}}\Delta E_{\mathrm{s}}$$
$$\text{s.t.} \begin{cases} \sum_{i\in S^{\mathrm{B}}} \tilde{h}_i(x_i) - \Delta E_{\mathrm{b}} + \Delta E_{\mathrm{s}} \le E_0 \\ \sum_{i\in S^{\mathrm{B}}} \widetilde{M}_i x_i \le b_{\mathrm{BR}} \\ \sum_{i\in S^{\mathrm{B}}} \tilde{A}_i x_i = b_{\mathrm{PF}} \\ x_i \in \chi_i, i \in S^{\mathrm{B}}. \\ (12)(13) \end{cases} \tag{16}$$

Let $x_0 = [\Delta E_{\mathrm{b}}; \Delta E_{\mathrm{s}}]$, $b_{\mathrm{E}} = E_0$, $c_0 = [\pi_{\mathrm{b}}; -\pi_{\mathrm{s}}]$, $D_0 = [-1, 1]$, $\chi_0 = \{x_0 | (12)(13)\}$, $\tilde{A}_0 = \boldsymbol{0}$, $\widetilde{M}_0 = \boldsymbol{0}$, $\tilde{h}_0(x_0) = D_0 x_0$ and $g_0(x_0) = c_0 x_0$, then (16) can be further rewritten as

$$\min \sum_{i\in S^{\mathrm{B}}\cup\{0\}} g_i(x_i)$$
$$\text{s.t.} \begin{cases} \sum_{i\in S^{\mathrm{B}}\cup\{0\}} \tilde{h}_i(x_i) \le b_{\mathrm{E}} \\ \sum_{i\in S^{\mathrm{B}}\cup\{0\}} \widetilde{M}_i x_i \le b_{\mathrm{BR}} \\ \sum_{i\in S^{\mathrm{B}}\cup\{0\}} \tilde{A}_i x_i = b_{\mathrm{PF}} \\ x_i \in \chi_i, i \in \{0\} \cup S^{\mathrm{B}}. \end{cases} \tag{17}$$

Let $\psi_0(x_0) = \left[\tilde{h}_0(x_0) - b_{\mathrm{E}}; \widetilde{M}_0\right]$, $A_0(x_0) = \tilde{A}_0$. And for $i \in S^{\mathrm{B}}$, let $\psi_i(x_i) = \left[\tilde{h}_i(x_i); \widetilde{M}_i x_i - b_{\mathrm{BR}}^i\right]$, $A_i(x_i) = \left[\tilde{A}_i x_i - b_{\mathrm{PF}}^i\right]$, where $\sum_{i\in S^{\mathrm{B}}} b_{\mathrm{BR}}^i = b_{\mathrm{BR}}$, $\sum_{i\in S^{\mathrm{B}}} b_{\mathrm{PF}}^i = b_{\mathrm{PF}}$. (17) can be reformulated as

$$\min \sum_{i\in S^{\mathrm{B}}\cup\{0\}} g_i(x_i)$$
$$\text{s.t.} \begin{cases} \sum_{i\in S^{\mathrm{B}}\cup\{0\}} \psi_i(x_i) \le 0 \\ \sum_{i\in S^{\mathrm{B}}\cup\{0\}} A_i(x_i) = 0 \\ x_i \in \chi_i, i \in \{0\} \cup S^{\mathrm{B}} \end{cases} \tag{18}$$

We note that, in (18), $i = 0$ can be viewed as a central coordinator, which only knows the total emission allowance of CO_2. And theoretically, all information in b_{E}, b_{BR}, b_{PF} can be assign to any one or more blocks in $\{0\} \cup S^{\mathrm{B}}$ for privacy protection.

B. Methodology

Let $|\pi| = n + 1$ and $\pi = \{\mathcal{A}_0, \mathcal{A}_1, \mathcal{A}_2, \dots, \mathcal{A}_n\}$ is a partition of the set $S^{\mathrm{B}} \cup \{0\}$, i.e., $\emptyset \notin \pi$, $\cup_{\mathcal{A}_j\in\pi, j=0,\cdots,n} \mathcal{A}_j = S^{\mathrm{B}} \cup \{0\}$, and $(\forall \mathcal{A}, \mathcal{B} \in \pi)\mathcal{A} \ne \mathcal{B} \Rightarrow \mathcal{A} \cap \mathcal{B} = \emptyset$.

Then we have the partition-based Lagrangian dual function of (18) is

$$h(\lambda; v) = \sum_{j=0}^{n} h_j(\lambda; v) \tag{19}$$

where $h_j(\lambda; v) = \inf_{(x_i\in\chi_i, i\in\mathcal{A}_j)} \left\{\sum_{i\in\mathcal{A}_j} g_i(x_i) + \left\langle \sum_{i\in\mathcal{A}_j} \psi_i(x_i), \lambda \right\rangle + \left\langle \sum_{i\in\mathcal{A}_j} A_i(x_i), v \right\rangle\right\}$, $\lambda \ge 0$, and v are Lagrangian multiplier vectors associated with constraints, "$\langle\cdot,\cdot\rangle$" denotes the inner product.

Let $y = (\lambda; v)$, then, the dual problem of (18) is

$$\max h(y). \tag{20}$$

This problem can be rewritten to be a minimization problem with local variables z_i and a common consensus variable y [35]:

$$\min\left\{-\sum_{j=0}^{n} h_j(z_j)\right\}$$
$$\text{s.t. } y - z_j = 0, j = 0, \dots, n \tag{21}$$

Partitioning the multiplier vector $p = (p_0, \cdots, p_n)$ and giving $\rho > 0$, the ADMM solving (21) consists of the iterations:

$$y^{k+1} := \underset{y}{\operatorname{argmin}} \left\{\left\langle \sum_{j=0}^{n} p_j^k, y \right\rangle + \frac{\rho}{2}\sum_{j=0}^{n} \left\| y - z_j^k \right\|^2\right\} \tag{22}$$

$$z_j^{k+1} := \underset{z_j}{\operatorname{argmin}} \left\{-h_j(z_j) - \left\langle p_j^k, z_j \right\rangle + \frac{\rho}{2}\left\| y^{k+1} - z_j \right\|^2\right\} \tag{23}$$

$$p_j^{k+1} := p_j^k + \rho\left(y^{k+1} - z_j^{k+1}\right). \quad (24)$$

The y-update problem (22) is minimizing a convex quadratic function of y, we can get the minimize y from the optimality condition, i.e.,

$$y^{k+1} = \frac{1}{n+1}\sum_{j=0}^{n} z_j^k - \frac{1}{(n+1)\rho}\sum_{j=0}^{n} p_j^k \quad (25)$$

By substituting the expression for $h_j(z_j)$ into z_j -update problem (23), we can obtain that

$$\begin{aligned}
&\inf_{z_j=\left(\lambda_{z_j};v_{z_j}\right),\lambda_{z_j}\geq 0}\Big\{-\inf_{(x_i\in\chi_i,i\in\mathcal{A}_j)}\Big\{\sum_{i\in\mathcal{A}_j} g_i(x_i) + \\
&\quad \langle\lambda_j, \sum_{i\in\mathcal{A}_j}\psi_i(x_i)\rangle + \langle v_j, \sum_{i\in\mathcal{A}_j} A_i(x_i)\rangle\Big\} - \langle p_j^k, z_j\rangle + \\
&\quad \frac{\rho}{2}\left\|y^{k+1} - z_j\right\|^2\Big\} = \\
&\sup_{z_j=\left(\lambda_{z_j};v_{z_j}\right),\lambda_{z_j}\geq 0}\inf_{(x_i\in\chi_i,i\in\mathcal{A}_j)}\Big\{\sum_{i\in\mathcal{A}_j} g_i(x_i) + \\
&\quad \langle z_j, \left(\sum_{i\in\mathcal{A}_j}\psi_i(x_i)\,; \sum_{i\in\mathcal{A}_j} A_i(x_i)\right) + p_j^k\rangle - \frac{\rho}{2}\left\|y^{k+1} - \right. \\
&\quad \left. z_j\right\|^2\Big\} = \\
&\inf_{(x_i\in\chi_i,i\in\mathcal{A}_j)}\sup_{z_j=\left(\lambda_{z_j};v_{z_j}\right),\lambda_{z_j}\geq 0}\Big\{\sum_{i\in\mathcal{A}_j} g_i(x_i) + \\
&\quad \langle z_j, \left(\sum_{i\in\mathcal{A}_j}\psi_i(x_i)\,; \sum_{i\in\mathcal{A}_j} A_i(x_i)\right) + p_j^k\rangle - \frac{\rho}{2}\left\|y^{k+1} - \right. \\
&\quad \left. z_j\right\|^2\Big\} \quad (26)
\end{aligned}$$

For any fixed $\{x_i \in \chi_i, i \in \mathcal{A}_j\}$, the minimum on the "sup{·}" in the right-hand side of (26) is uniquely attained by

$$z_j = \begin{bmatrix}\lambda_{z_j}\\ v_{z_j}\end{bmatrix} = \begin{bmatrix}\max\left\{0, \lambda_{y^{k+1}} + \frac{1}{\rho}\left(\sum_{i\in\mathcal{A}_j}\psi_i(x_i) + \lambda_{p_j^k}\right)\right\}\\ v_{y^{k+1}} + \frac{1}{\rho}\left(\sum_{i\in\mathcal{A}_j} A_i(x_i) + v_{p_j^k}\right)\end{bmatrix}. \quad (27)$$

We may thus substitute (27) into the function on the right-hand side of (26) to eliminate the variables z_j. Then, we can obtain

$$\begin{aligned}
\{x_i^*, i\in\mathcal{A}_j\} := \operatorname{argmin}_{(x_i\in\chi_i,i\in\mathcal{A}_j)}\Bigg\{&\sum_{i\in\mathcal{A}_j} g_i(x_i) + \\
&\frac{\rho}{2}\left\|\left[\begin{matrix}\max\left\{0, \lambda_{y^{k+1}} + \frac{1}{\rho}\left(\sum_{i\in\mathcal{A}_j}\psi_i(x_i) + \lambda_{p_j^k}\right)\right\}\\ v_{y^{k+1}} + \frac{1}{\rho}\left(\sum_{i\in\mathcal{A}_j} A_i(x_i) + v_{p_j^k}\right)\end{matrix}\right]\right\|^2\Bigg\} \quad (28)
\end{aligned}$$

That is to say, $\{x_i^*, i \in \mathcal{A}_j\}$ is a solution of the following problem:

$$\begin{aligned}
&\min \sum_{i\in\mathcal{A}_j} g_i(x_i) + \frac{\rho}{2}\left\|\left[v_{y^{k+1}} + \frac{1}{\rho}\left(\sum_{i\in\mathcal{A}_j} A_i(x_i) + v_{p_j^k}\right)\right]\right\|^2 \\
&\text{s.t.}\begin{cases}\tau \geq 0\\ \tau \geq \left[\lambda_{y^{k+1}}\right] + \frac{1}{\rho}\left(\sum_{i\in\mathcal{A}_j}\psi_i(x_i) + \lambda_{p_j^k}\right)\\ x_i \in \chi_i, i\in\mathcal{A}_j\end{cases} \quad (29)
\end{aligned}$$

It is not difficult to verify that (29) is strictly convex, then, the unique solution $\{x_i^*, i \in \mathcal{A}_j\}$ can be found. Therefore, z_j can be determined by (27).

Note that, by the separability of problem (21), the updates (27) and (24) can be performed in parallel for our partition $\pi = (\mathcal{A}_j, j = 0,1,\dots,n)$. Now, we give our preliminary (unimproved) dual ADMM based on partition (DADMM-P) in full details.

Algorithm 1

Initialization: $z_j^0, p_j^0, M > 0, \rho > 0, \varepsilon^{\text{feasible}} > 0$.
for $k = 0, \dots, M$
  (25);
  for each sub set of units $j = 0, \dots, n$:(in parallel)
    Obtain $\{x_i^*, i \in \mathcal{A}_j\}$ by solving (29);
    z_j^{k+1} = (27);
    (24);
  end
  if $\varepsilon := \|y^{k+1} - y^k\|_\infty < \varepsilon^{\text{feasible}}$ **break**;
end.

As shown in Fig. 1, $\mathcal{A}_0$ is equivalent to a central coordinator that coordinates subsystems. Each subsystem only communicates with the coordinator and there are no direct communication links between the subsystems. In addition, algorithm 1 can be improved in computing efficiency by reducing coupling constraints and employing the new update step of multiplier. We will give these improvements and some discussion about the advantage of our method in needing less public information in the following subsections.

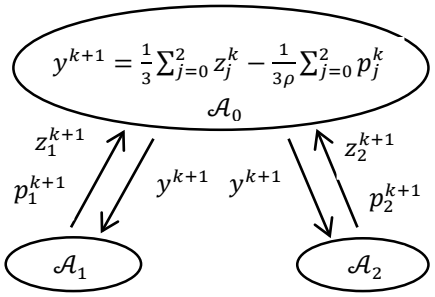

Fig. 1. Communication strategy for our proposed method.

C. Reducing Coupling Constraints

As can be seen in Section III.A, $\sum_{i\in S^{\text{B}}\cup\{0\}}\psi_i(x_i) \leq 0$ and $\sum_{i\in S^{\text{B}}\cup\{0\}}\tilde{A}_i x_i = b_{\text{PF}}$ can be viewed as "coupling constraints" because that each this coupling constraint will lead to an element in consensus variable y of (21). In order to obtain better convergence for our proposed DADMM-P, we should reduce the number of coupling constraints to a minimum.

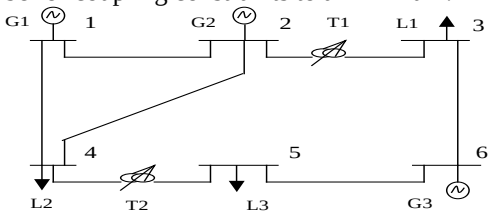

Fig. 2. 6-bus system.

A 6-bus system shown in Fig. 2 is used as an example to illustrate the procedure of identifying "real" coupling constraints. The 6-bus system is divided into three subsystems, i.e., $\pi = \{\{\mathcal{A}_0 = \{0\}, \mathcal{A}_1 = \{1,2,4\}, \mathcal{A}_2 = \{3,5,6\}\}$. Fig. 3 gives the coefficient matrix and RHS for $\sum_{i\in S^{\text{B}}\cup\{0\}}\tilde{A}_i x_i = b_{\text{PF}}$. It can be seen that we have $v \in R^{6T}$ in consensus variable y. However, bus 1 in subsystem $\mathcal{A}_1$ have no association with subsystem $\mathcal{A}_2$, and bus 6 in subsystem $\mathcal{A}_2$ is not association with subsystem $\mathcal{A}_1$. So $A_1^{\text{r}} \cdot [x_1; x_2; x_4] - \boldsymbol{P}_1^{\text{D}} \leq 0$ can be moved from coupling constrains $\sum_{i\in S^{\text{B}}}\tilde{A}_i x_i = b_{\text{PF}}$ to decoupling constraint sets χ_1. Similarly, $A_2^{\text{r}} \cdot [x_3; x_5; x_6] - \boldsymbol{P}_6^{\text{D}} \leq \boldsymbol{0}$ can be

moved to decoupling constraint sets χ_2. Then, the reduced coupling constraints for DC power flower equation are $[\tilde{A}_0^r, \tilde{A}_1^r, \tilde{A}_2^r][x_0; x_1; x_2; x_4; x_3; x_5; x_6] - [\boldsymbol{P}_2^{\mathrm{D}}; \boldsymbol{P}_4^{\mathrm{D}}; \boldsymbol{P}_3^{\mathrm{D}}; \boldsymbol{P}_5^{\mathrm{D}}] \leq \mathbf{0}$. Now, we have $v \in R^{4T}$ in consensus variable y. The reduction of elements in consensus variable will accelerate the convergence of the proposed method (As can be seen in Fig. 6 of section IV).

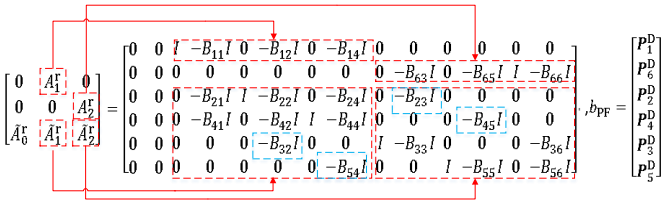

Fig. 3. $\sum_{i \in S^{\mathrm{B}} \cup \{0\}} \tilde{\boldsymbol{A}}_i \boldsymbol{x}_i = \boldsymbol{b}_{\mathbf{PF}}$ for the 6-bus system.

D. Analysis of Public Information

As discussed in Section I, while solving the subproblem corresponding to a subsystem, all the information which does not belong to the current subsystem are regarded as public information. A 6-bus system shown in Fig. 2 is used as an example to illustrate the public information. Fig. 3 and Fig. 4 give the coefficient matrix of $\sum_{i \in S^{\mathrm{B}} \cup \{0\}} \tilde{A}_i x_i = b_{\mathrm{PF}}$ for our method and one for method in [7], respectively. Similarly, $\pi = \{\{\mathcal{A}_0 = \{0\}, \mathcal{A}_1 = \{1,2,4\}, \mathcal{A}_2 = \{3,5,6\}\}$. As shown in Fig. 3, B_{32} and B_{23} are the admittance information of the same branch. Similarly, B_{54} and B_{45} are the admittance information of the same branch. In Fig. 4, on the basis of knowing the boundary branch admittance B_{23}, B_{32}, B_{54} and B_{45}, $\mathcal{A}_1$ needs to know the buses admittances B_{33} and B_{55} in $\mathcal{A}_2$, which are private information for $\mathcal{A}_2$. Similarly, $\mathcal{A}_2$ needs to know the boundary branches admittances B_{23}, B_{32}, B_{54}, B_{45} and the private buses admittance B_{22} and B_{44} in $\mathcal{A}_1$. According to the discussion, compared to the method in [7] (Fig. 4), we know that there is less information disclosed between adjacent subsystems in our method (Fig. 3).

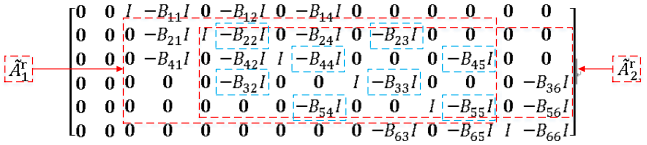

Fig. 4. Public information for method in [7].

E. Improving the Update Step of Multiplier

Numerical results show that the convergence rate of the Peaceman-Rachford splitting method (PRSM) is faster than ADMM when it is convergent [31]. In [31], a strictly contractive PRSM is proposed. Similar to [31], we can obtain the new multiplier update step,

$$p_j^{k+\frac{1}{2}} := p_j^k + \mu\rho\left(y^{k+1} - z_j^k\right), \tag{30}$$

$$p_j^{k+1} := p_j^{k+\frac{1}{2}} + \mu\rho\left(y^{k+1} - z_j^{k+1}\right). \tag{31}$$

where $\mu \in (0, 1)$ is underdetermined relaxation factor.

In Algorithm 1, to adopt this new multiplier update step, we can insert (30) before (27) and simultaneously substitute (31) for (24) which following (27). Then the obtained algorithm is our improved DADMM-P denoted as Algorithm 2.

IV. Numerical Case Studies

The proposed algorithm is implemented using MATLAB on a desktop with an Intel Core i7-8700K CPU and 8GB of RAM. Problem (29) is solved by Cplex 12.6.2. All the codes and cases of the simulations for this paper can be freely downloaded from https://github.com/linfengYang/Dual-Consensus-ADMM-for-DC-OPF-CET.

$T = 24$, $\pi_{\mathrm{b}} = 12$, $\pi_{\mathrm{s}} = 10$, and $M = 4000$. $r_k = [y^k - z_1^k; \ldots; y - z_n^k]$ is the primal residual at iteration k. $s_k = -\rho[z_1^k - z_1^{k-1}; \ldots; z_n^k - z_n^{k-1}]$ is the dual residual. Unless otherwise specified, the calculation results of this section are all obtained after reducing coupling constraints.

A. 6-Bus System

The detailed data of the 6-bus system which includes 3 generators and 3 loads, just as shown in Fig. 2, can be found in [36]. In Case 1, the 6-bus system is divided into three subsystems, i.e., $\pi = \{\mathcal{A}_0 = \{0\}, \mathcal{A}_1\{1,2,4\}, \mathcal{A}_2 = \{3,5,6\}\}$. In Case 2, the 6-bus system is divided into seven subsystems, i.e., $= \{\{\mathcal{A}_0 = \{0\}, \mathcal{A}_1 = \{1\}, \mathcal{A}_2 = \{2\}, \mathcal{A}_3 = \{3\}, \mathcal{A}_4 = \{4\}, \mathcal{A}_5 = \{5\}, \mathcal{A}_6 = \{6\}\}$. Then, the number of elements in consensus variable is $8T$ in Case 1 and $20T$ in Case 2. $E_0 = 600$, $\Delta E_{\mathrm{b}}^{\max} = 10000$, $\Delta E_{\mathrm{s}}^{\max} = 600$, and $\varepsilon^{\mathrm{feasible}} =$1e-5.

Table I
The results of two cases for 6-bus system

Case	ρ	F_{TC}	$\|r_k\|_2$	$\|s_k\|_2$	RG	N_{it}
1	0.25	1.430141e+5	1.15e-4	1.73e-5	5.87E-05	1114
2	0.14	1.430133e+5	1.95e-4	6.43e-6	4.62E-05	3132

For this 6-bus system, the result obtained by using Cplex to solve (18) directly is $F_{\mathrm{TC}}^{\mathrm{Cplex}} =$1.430057e+5. The computing results of our improved DADMM-P for two cases of 6-bus system are listed in Table I. In this table, the results in column labeled "RG" are relative gap between the results obtained by Cplex and the ones obtained by our method. And they can be calculated by $\left|F_{\mathrm{TC}} - F_{\mathrm{TC}}^{\mathrm{Cplex}}\right| / F_{\mathrm{TC}}^{\mathrm{Cplex}}$, which can be used to evaluate the solution quality of the proposed algorithm. The column labeled "N_{it}" represents the total number of iterations required to solve the current optimization. Table I shows that our DADMM-P method obtains almost the same solutions for two cases and these solutions are nearly equal to the solution obtained by Cplex. And the last column of Table I shows that the fewer elements the consensus variable has, the more efficient the DADMM-P converges.

B. 30-Bus System

Table II
The coefficients of 30-bus system

Gen	α	β	γ	a	b	c
1	10	0.02	0.0002	11.50486	-0.15586	0.00194
2	10	0.015	0.00024	11.50486	-0.15586	0.00194
3	20	0.018	0.00008	13.86	0.33	0.0042
4	10	0.01	0.00012	13.3056	0.3168	0.00403
5	20	0.018	0.00008	13.86	0.33	0.0042
6	10	0.015	0.0002	11.50486	-0.15586	0.00194

The 30-bus system includes 6 generators and 21 loads is given in Fig. 5. The coefficients of generators for this system are listed in Table II. The data of emission coefficients are taken from [37] and reduced in proportion. In this subsection,

$E_0 = 600$, $\Delta E_{\mathrm{b}}^{\max} = 10000$, $\Delta E_{\mathrm{s}}^{\max} = 600$, and $\varepsilon^{\text{feasible}} = 1\mathrm{e}-5$.

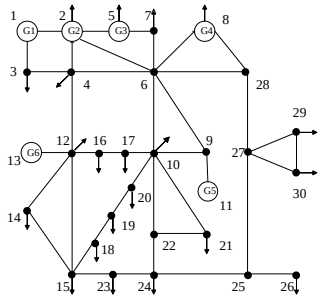

Fig. 5. 30-bus system.

At first, in Table III, we give the comparison of public information between our method and [7]. Also, the numbers of elements in consensus variable are given. Obvious, the number of public information of our method is significantly lesser than that in [7]. In addition, our method is easier to calculate the number of the public information. Our method only needs to know the number of the boundary branches between adjacent subsystems to calculate the number of the public information while [7] also need to consider partition strategy on the basis of knowing the number of the boundary branches.

Table III
Comparison of public information

Case	Subsystems $\mathcal{A}_n$	# of public information for the method in [7]	# of public information for our method	# of elements in consensus variable
1	$\mathcal{A}_1 = \{1{:}8, 25{:}30\}$ $\mathcal{A}_2 = \{9{:}24\}$	11	**4**	15T
2	$\mathcal{A}_1 = \{1{:}8, 25{:}30\}$ $\mathcal{A}_2 = \{9{:}20\}$ $\mathcal{A}_3 = \{21{:}24\}$	18	**7**	25T
3	$\mathcal{A}_1 = \{1{:}8\}$ $\mathcal{A}_2 = \{9{:}20\}$ $\mathcal{A}_3 = \{21{:}24\}$ $\mathcal{A}_4 = \{25{:}30\}$	22	**9**	31T
4	$\mathcal{A}_1 = \{1{:}10\}$ $\mathcal{A}_2 = \{11{:}20\}$ $\mathcal{A}_3 = \{21{:}30\}$	23	**9**	32T

The computation results of unimproved DADMM-P (without new multiplier update step) for four cases of 30-bus system are listed in Table IV. The result obtained by using Cplex for this system is 5.174874e+4. Table III and Table IV show that the more elements the consensus variable has, the more iterations the algorithm often does. Thus, a useful guidance for dividing the entire system into subsystems is the number of element in consensus vector.

Table IV
Results of four cases for 30-bus system

Case	ρ	F_{TC}	$\|r_k\|_2$	$\|s_k\|_2$	RG	N_{it}
1	0.49	5.174889e+4	2.24e-4	2.03e-5	2.90e-6	380
2	0.39	5.174896e+4	7.40e-4	1.86e-5	4.25e-6	622
3	0.34	5.174890e+4	1.89e-3	2.55e-5	3.09e-6	836
4	0.38	5.174887e+4	5.45e-4	2.13e-5	2.51e-6	775

Furthermore, for case 1, the numbers of iterations of Algorithm 1 with coupling constraints reduction (Labeled "Improved") and without reduction (Labeled "Unimproved") were given in Fig. 6. This figure shows that reducing coupling constraints can indeed reduce the number of iterations for most of values of ρ.

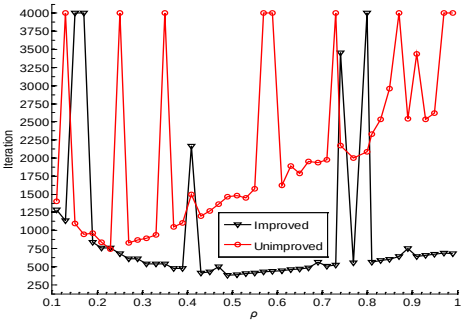

Fig. 6. Comparison of coupling constraints reduction (Case 1)

For different ρ, the numbers of iterations of Algorithm 1 while solving case 1-4 are given in Fig. 7. This figure shows that, for most values of ρ, the number of elements in consensus variable and the number of iterations are positively correlated. Fig. 7 also shows that improper ρ could lead to a slow convergence. In addition, in order to obtain best convergence performance for different systems, ρ often should be different, just as shown in Table IV. Thus, it can't give a unique value for ρ that would be best for all practical problems [38]. Our experiences show that setting ρ in the range of 0.3-0.55 is usually proper for different partitions of the 30-bus system.

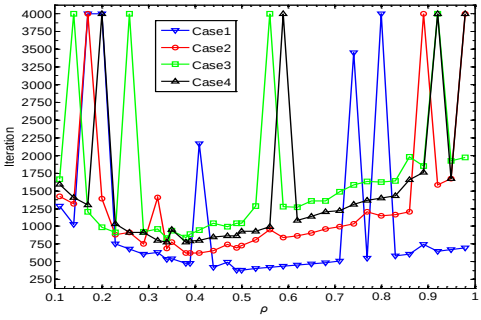

Fig. 7. Impact of $\boldsymbol{\rho}$ on the convergence rate

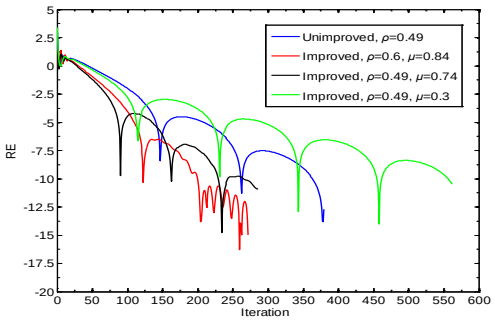

Fig. 8. Two type of update steps for multiplier (Case 1)

Let $\mathrm{RE} = \log\|\mathrm{RG}\|_2$, for case 1, Fig. 8 gives "RE" for Algorithm 1 (Labeled "Unimproved") and Algorithm 2 with different ρ and μ (Labeled "Improved, …"). In this figure, 0.49 is the best choice for ρ in Algorithm 1. $\rho = 0.6$ and $\mu = 0.84$ is the best choices for Algorithm 2. This figure shows, with proper ρ and μ, the new multiplier update step can improve the convergence performance of DADMM-P. But, improper choice of μ may instead be exacerbating the convergence performance.

The computation results of DADMM-P with new multiplier update step are listed in Table V. Table IV and Table V show that the number of iterations is significantly reduced in all cases when the new update step of multiplier was employed. Moreover, the values of ρ leading to the best performance for the algorithm changed. The calculation time of four cases are 23.5 seconds, 59.7 seconds, 85.2 seconds and 67.8 seconds, respectively.

Table V
Results of four cases for 30-bus system after improving the update step of multiplier

Case	ρ	μ	F_{TC}	$\|r_k\|_2$	$\|s_k\|_2$	RG	N_{it}
1	0.6	0.84	5.174875e+4	8.46e-4	3.27e-5	1.93e-7	272
2	0.3	0.70	5.174903e+4	7.61e-4	1.01e-5	5.60e-6	559
3	0.4	0.71	5.174932e+4	6.43e-4	2.44e-5	1.12e-5	727
4	0.39	0.75	5.174884e+4	3.13e-4	3.58e-5	1.93e-6	580

For different μ, Fig. 9 gives the number of iterations for Algorithm 2 (Labeled "…, Improved, …"). In this figure, the dotted line represents the fewest iterations for Algorithm 1 (Labeled "…, Unimproved, …"). Our experience shows that μ in the range of 0.5-0.85 is usually proper for the 30-bus system.

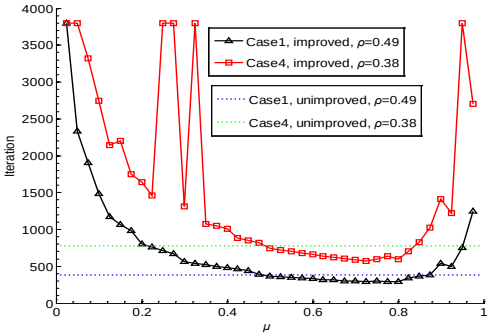

Fig. 9. Results for the new update step for multiplier under different $\boldsymbol{\mu}$

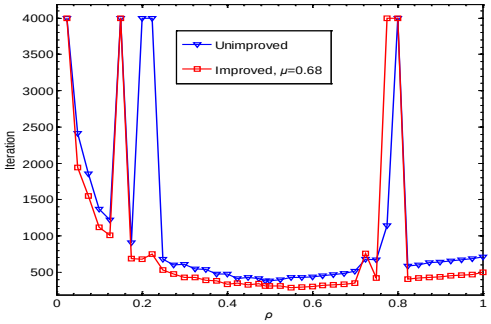

Fig. 10. The number of iterations with $\boldsymbol{\mu = 0.68}$ and different $\boldsymbol{\rho}$ (Case 1)

For Case 1, Fig. 10 gives the number of iterations of our method with $\mu = 0.68$ and different ρ. In this figure, the lines with label "Unimproved" and "Improved, …" report the results for Algorithm 1 and Algorithm 2 respectively. And this figure shows that a good choice of μ often can improve the performance of the algorithm for most ρ.

When ρ is 0.2 or 0.8, we can see from Fig. 7 and Fig. 10 that Algorithm 1 does not converge while solving Case 1. For this situation, Fig. 11 gives the numbers of iterations for Algorithm 1 (Labeled "Unimproved") and Algorithm 2 (Labeled "Improved, …"). This figure shows that the number of iterations is reduced significantly after using improved multiplier update step. In addition, for all ρ, our proposed method can become converged after improving the multiplier update step.

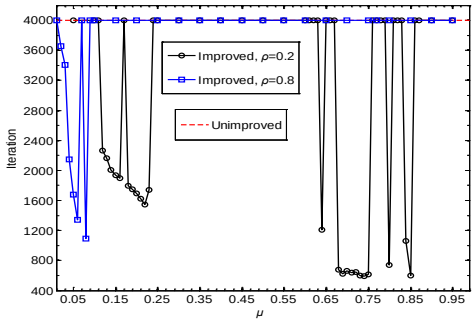

Fig. 11. Comparison of unimproved and improved with $\boldsymbol{\rho}$ of 0.2 and 0.8 (Case 1).

C. *600-bus system*

As illustrated in Section IV-B, the general guiding principle for partitioning subsystem is to include fewer elements in consensus convector. To further verify this partitioning subsystem guidance, a 600-bus system shown in Fig. 12 is tested via our algorithm. The 600-bus system includes 20 subsystems and each subsystem is 30-bus system used in Section IV-B. The first subsystem contains bus 1 to the bus 30, and the second subsystem contains bus 31 to the bus 60, and so on. $E_0 = 12000$, $\Delta E_{\mathrm{b}}^{\max} = 200000$, and $\Delta E_{s}^{\max} = 12000$.

The 600-bus system is divided into five subsystems and contains 3 tie lines as shown in Fig. 12. The calculate result of Cplex for 600-bus system is 1.01650482e+06.

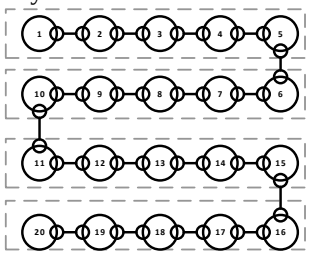

Fig. 12. 600-bus system.

Table VI
Comparison of public information

Subsystems $\mathcal{A}_n$	# of public information for the method in [7]	# of public information for our method	# of the number of element in consensus vector
$\mathcal{A}_1 = \{1{:}150\}$ $\mathcal{A}_2 = \{151{:}300\}$ $\mathcal{A}_3 = \{301{:}450\}$ $\mathcal{A}_4 = \{451{:}600\}$	9	**3**	$12T$

Table VII
Comparison of Algorithm 1 and 2 for 600-bus system

Algorithm	ρ	μ	F_{TC}	$\|r_k\|_2$	$\|s_k\|_2$	RG	N_{it}
1	25	None	1.01652102e+6	1.48e-4	6.03e-3	1.59e-5	2260
2	25	0.8	1.01650945e+6	1.79e-4	4.01e-3	4.55e-6	1568

Table VI gives the comparison of public information between our method and the method in [7]. Table VII gives the results for Algorithm 1 and Algorithm 2. The $\varepsilon^{\mathrm{feasible}}$ are 4e-5 and 3e-5 for Algorithm 1 and Algorithm 2 respectively. As can be seen in Table VII, Algorithm 2 obtain higher quality solution with fewer iterations. This again confirms that improving the update step of multiplier is efficient.

In Addition, after weighing all experiment data, it seems that the value of ρ increases (decreases) along with the increasing (decreasing) of system size, and it increases (decreases) along with the decreasing (increasing) of the number of subsystems or the number of element in consensus variable.

V. Conclusion

This paper discusses a fully distributed ADMM algorithm for solving the DC-OPF-CET. Since DC-OPF-CET problem is a convex programming with linear constraints and nonlinear constraints, our proposed algorithm can guarantee the global optimal solutions. Compared to most other ADMM-based distributed approaches, such as the algorithm in [7], which disclosing boundary buses and branches information among adjacent subsystems, our proposed algorithm adopts a new strategy which making it only needs disclosing boundary branches among adjacent subsystems. Simply, our algorithm needs significantly less public information than other ADMM-based methods, and it is more suitable for competitive electricity market when the privacy protection becoming more and more important. We improve convergence speed of our method further by reducing the coupling constraints and employing an improved update step of multiplier. We introduce subsystem indexed 0 to deal with CET and regard this subsystem as a central coordinator although any of the divided subsystems can be treated as central coordinator and all the private data in the RHS of the constraints can be distributed to any subsystems.

We focus on the impact of parameter ρ, μ, the number of elements in consensus variable, the number of subsystems and the scale of power systems on the convergence performance in this paper. The numerical case studies contain a 6-bus system, a 30-bus system, and a 600-bus system. Results show that the convergence performance largely depends on the number of elements in consensus variable rather than the number of subsystems or the scale of power systems. Numerical results also confirm that our proposed two improvements can indeed improve computation efficiency, especially when applied to large-scale power systems. Therefore, an excellent subsystem partition strategy could enhance the convergence performance, since it has fewer numbers of global variables.

References

[1] J. Carpentier, "Contribution à l'étude du dispatching économique," *Bull. Soc. Françai se D'Electricité*., 1962.

[2] J. A. Momoh and J. Z. Zhu, "Improved interior point method for OPF problems," *IEEE Trans. Power Syst.*, vol. 14, no. 3, pp. 1114-1120, Aug. 1999.

[3] J. Lavaei and S. H. Low, "Zero Duality Gap in Optimal Power Flow Problem," *IEEE Trans. Power Syst.*, vol. 27, no. 1, pp. 92-107, Feb. 2012.

[4] H. Wang, C. E. Murillo-Sanchez, R. D. Zimmerman and R. J. Thomas. "On Computational Issues of Market-Based Optimal Power Flow", *IEEE Trans. Power Syst*., vol. 22, no. 3, pp. 1185-1193, Aug. 2007.

[5] T. Erseghe, "Distributed optimal power flow using admm," *IEEE Trans. Power Syst.*, vol. 29, no. 5, pp. 2370–2380, Sept. 2014.

[6] A. Kargarian, J. Mohammadi, J. Guo, S. Chakrabarti, M. Barati, G. Hug, S. Kar and R. Baldick, "Toward Distributed/Decentralized DC Optimal Power Flow Implementation in Future Electric Power Systems," *IEEE Trans. Smart Grid*, 2016.

[7] Y. Wang, L. Wu and S. Wang, "A Fully-Decentralized Consensus-Based ADMM Approach for DC-OPF With Demand Response", *IEEE Trans. Smart Grid*, vol. 8, no. 6, pp. 2637-2647, Nov. 2017.

[8] Z. Liang, S. Lin and M. Liu, "Distributed Optimal Power Flow of AC/DC Interconnected Power Grid Using Synchronous ADMM," *IOP Conference Series: Materials Science and Engineering*, vol. 199, no. 1, 2017.

[9] A. Kargarian, Y. Fu, S. DorMohammadi, and M. Rais-Rohani, "Optimal operation of active distribution grids: a system of systems framework," *IEEE Trans. Smart Grid*, vol. 5, no. 3, pp. 1228–1237, May. 2014.

[10] A. Kargarian, Y. Fu, and Z. Li, "Distributed security-constrained unit commitment for large-scale power systems," *IEEE Trans. Power Syst.*, vol. 30, no. 4, pp. 1925–1936, July. 2015.

[11] A. Ahmadi-Khatir, A. Conejo, and R. Cherkaoui, "Multi-area unit scheduling and reserve allocation under wind power uncertainty," *IEEE Trans. Power Syst.*, vol. 29, no. 4, pp. 1701–1710, July. 2014.

[12] K. Chung, B. Kim, and D. Hur, "Distributed implementation of generation scheduling algorithm on interconnected power systems," *Energy Conversion and Management*, vol. 52, no. 12, pp. 3457–3464, 2011.

[13] G. Hug-Glanzmann and G. Andersson, "Decentralized optimal power flow control for overlapping areas in power systems," *IEEE Trans. Power Syst.*, vol. 24, no. 1, pp. 327–336, Feb. 2009.

[14] F. Nogales, F. Prieto, and A. Conejo, "A decomposition methodology applied to the multi-area optimal power flow problem," *Ann. Oper. Res.*, vol. 120, pp. 99–116, 2003.

[15] A. Bakirtzis and P. Biskas, "A decentralized solution to the DC-OPF of interconnected power systems," *IEEE Trans. Power Syst.*, vol. 18, no. 3, pp. 1007–1013, Aug. 2003.

[16] A. Dimakis, S. Kar, J. Moura, M. Rabbat, and A. Scaglione, "Gossip algorithms for distributed signal processing," *Proceedings of the IEEE*, vol. 98, no. 11, pp. 1847–1864, Nov. 2010.

[17] S. Yang, S. Tan, and J. Xu, "Consensus based approach for economic dispatch problem in a smart grid," *IEEE Trans. Power Syst.*, vol. 28, no. 4, pp. 4416–4426, Nov. 2013.

[18] M. Ma, L. Fan and Z. Miao, "Consensus ADMM and Proximal ADMM for economic dispatch and AC OPF with SOCP relaxation," *North American Power Symposium*, 2016.

[19] S. Magnusson, P. Weeraddana, and C. Fischione, "A distributed approach for the optimal power flow problem based on admm and sequential convex approximations," *IEEE Trans. Control of Net. Syst.*, vol. 2, no. 3, pp. 238–253, Sept. 2015.

[20] M. Kraning, E. Chu, J. Lavaei, and S. Boyd, "Dynamic network energy management via proximal message passing," *Foundations and Trends in Optimization*, vol. 1, no. 2, pp. 70–122, 2013.

[21] A. Sun, D. Phan, and S. Ghosh, "Fully decentralized AC optimal power flow algorithms," *IEEE Power and Energy Society General Meeting*, July. 2013.

[22] Y. Xu, J. Hu, W. Gu, W. Su and W. Liu, "Real-Time Distributed Control of Battery Energy Storage Systems for Security Constrained DC-OPF," *IEEE Trans. on Smart Grid*, vol. 9, no. 3, pp. 1580-1589, May. 2018.

[23] G. Chen, C. Li and Z. Y. Dong, "Parallel and Distributed Computation for Dynamical Economic Dispatch," *IEEE Trans. Smart Grid*, vol. 8, no. 2, pp. 1026-1027, Mar. 2017.

[24] G. Chen and J. Y. Li, "A Fully Distributed ADMM-Based Dispatch Approach for Virtual Power Plant Problems," *Applied Mathematical Modelling*, vol. 58, pp. 300-312, June. 2018.

[25] P. Biskas, A. Bakirtzis, N. Macheras, and N. Pasialis, "A decentralized implementation of dc optimal power flow on a network of computers," *IEEE Trans. Power Syst.*, vol. 20, no. 1, pp. 25–33, Feb. 2005.

[26] Z. Li, Q. Guo, H. Sun, and J. Wang, "Coordinated economic dispatch of coupled transmission and distribution systems using heterogeneous decomposition," *IEEE Trans. Power Syst.*, vol. 31, no. 6, pp. 4817-4830, Nov. 2016.

[27] E. Dall'Anese, H. Zhu and G. B. Giannakis, "Distributed Optimal Power Flow for Smart Microgrids," *IEEE Trans. Smart Grid*, vol. 4, no. 3, pp. 1464-1475, Sept. 2013.

[28] S. Boyd, N. Parikh, E. Chu, B. Peleato and J. Eckstein, "Distributed Optimization and Statistical Learning via the Alternating Direction Method of Multipliers," *Now Foundations and Trends*, vol. 3, no. 1, pp. 1-128, 2011.

[29] D. Gabay and B. Mercier, "A dual algorithm for the solution of nonlinear variational problems via finite element approximation," *Computers & Mathematics with Applicaions*, vol. 2, no. 1, pp. 17–40, 1976.

[30] (Feb. 5, 2013). [Online]. Available: https://www.weforum.org/reports/energy-vision-2013-energy-transitions-past-and-future.

[31] H. Bingsheng, H. Liu, Z. Wang and X. Yuan, "A Strictily Contractive Peaceman-Rachford Splitting Method For Convex Programming," *Siam Journal on Optimization A Publication of the Society for Industrial and Applied Mathematics*, vol. 24, no. 3, pp. 1011-1040, 2014.

[32] S. Bisanovic, M. Hajro and M. Dlakic, "Unit commitment problem in deregulated environment," *International Journal of Electrical Power and Energy Systems*, vol. 42, no. 1, pp. 150-157, Nov. 2012.

[33] (Apr. 22, 2016) [Online]. Available: https://ec.europa.eu/clima/policies/international/negotiations/paris_en.

[34] I. Kockar, A. J. Conejo and J. R. Mcdonald, "Influence of the Emissions Trading Scheme on generation scheduling," *International Journal of Electrical Power and Energy Systems*, vol. 31, no. 9, pp. 465-473, 2009.

[35] M. Fukushima, "Application of the alternating direction method of multipliers to separable convex programming problems," *Computational Optimization and Applications*, vol. 1, no. 1, pp. 93-111, Jan. 1992.

[36] X. Bai and H. Wei, "Semi-definite programming-based method for security-constrained unit commitment with operational and optimal power flow constraints," *Iet Generation Transmission and Distribution*, vol. 3, no. 2, pp. 182-197, Feb. 2009.

[37] U. Güvenç, Y. Sönmez, S. Duman and N Yörükeren, "Combined economic and emission dispatch solution using gravitational search algorithm," *Scientia Iranica*, vol. 19, no. 6, pp. 1754-1762, 2012.

[38] E. Ghadimi, A. Teixeira, I. Shames, M. Johansson, "Optimal Parameter Selection for the Alternating Direction Method of Multipliers (ADMM): Quadratic Problems," *IEEE Trans. Automatic Control*, vol. 60, no. 3, pp. 644-658, Mar. 2015.